Kybernetik 15, 27—37 (1974)

Model of Brain Rhythmic Activity

The Alpha-Rhythm of the Thalamus

F. H. Lopes da Silva, A. Hoeks*, H. Smits, and L. H. Zetterberg

Brain Research Department, Institute of Medical Physics, National Health Research Council, T.N.O., Utrecht, The Netherlands and Department of Telecommunication Theory, Royal Institute of Technology, Stockholm, Sweden

Received: August 24, 1973

Abstract

1. A model of a neuronal network has been set up in a digital computer based on histological and biophysical data experimentally obtained from the thalamus; the model includes two populations of neurons interconnected by means of negative feedback; in the model allowance is also made for other sort of interactions.

2. To test the hypothesis that the alpha-rhythm (8–13 Hz rhythmic activity characteristic of the EEG) is a filtered noise signal the simulated neuronal network was stimulated by random trains of pulses with a Poisson distribution. The density of pulses fired by the simulated neurons was computed as well as the oscillations of the mean membrane potential of the population of simulated neurons. The latter was found to be equivalent to the experimentally obtained alpha rhythms.

3. In order to test the hypothesis that several noise sources are responsible for thalamo-cortical coherences three simulated neuronal networks were coupled together using several noise sources as secondary inputs. It was shown that although all the networks produced simulated alpha signals with identical spectra they could have significantly different values of coherence depending on the relation between correlated and uncorrelated input signals.

4. The model was analysed by means of linear systems analysis after introducing the necessary simplifications and approximations. In this way it was possible to evaluate the influence of different physiological or histological parameters upon the statistical properties of the resulting rhythmic activity in an analytical form.

5. By changing the model parameters it was shown that a family of spectral curves could be obtained which simulated the development of the EEG as function of age from a predominantly low frequency to a clearly rhythmic type of signal. This was shown to depend mainly on the feedback coupling parameters.

Introduction

The neural processes which are responsible for the generation of the electroencephalogram or EEG, are still far from being properly understood. Research carried out with the objective of clarifying those processes is of general importance because it attempts to answer the fundamental question of why and how synchrony can occur in populations of neurons. Furthermore, this line of research also has a practical side, because it may be assumed that a better understanding of the neurophysiology of EEG waves should lead to an improvement in the interpretation of EEG data both in clinical and physiological research.

The investigation reported here is an attempt to establish which are the basic mechanisms of generation of one of the most conspicuous EEG phenomena, the alpha-rhythm. This study has been carried out partly from a theoretical standpoint, but also experimentally.

1. The Hypothesis

Some of the experimental results obtained in the dog have been the object of a full report (Lopes da Silva *et al.*, 1973). They can be summarized as follows: alpha-rhythms have been recorded from cortical and thalamic areas using chronic indwelling electrodes while the eyes of the dogs were closed. The alpha-rhythms presented the characteristics of a bandpass filtered noise. Alpha-rhythms with the same peak frequency and bandwidth were recorded from both cortical and thalamic areas. However, correlations or coherences between related cortical areas were consistently larger than the thalamo-cortical coherences which have so far been obtained.

These results led us to formulate the hypothesis that alpha-rhythms may be assumed to be signals generated by neuron populations with frequency selective properties, when they are submitted to a random input. Thus neural networks with the same design and frequency selectivity may exist in different brain areas (cortical and thalamic).

These may give rise to alpha-rhythms with the same frequency spectra, but with variable coefficients of coherence, depending upon the correlation of the

* A part of this work has been submitted by A. Hoeks to the Technical University, Eindhoven in partial fulfilment of a M.Sc. in Engineering.

distinct network's random inputs. The characteristics of the alpha-rhythm would, therefore, depend upon

— the frequency selectivity properties of a neuronal population,

— the statistical properties of the input to such a population and

— gating mechanisms probably capable of setting the mode of activity of the neural networks, i.e. extrinsic modulating influences which may be responsible for the simultaneous occurrence of alpha-rhythms at different sites in the brain.

2. The Model

In this article, we shall limit ourselves to the research carried out to test the hypothesis presented above by use of a digital computer simulation of a neural network. Our attempt in this direction differs from that of others. On the one hand, we did not assume self-oscillating networks as have others (cf. review Rashevsky, 1971). On the other hand, our approach differed from that of Anderson *et al.* (1966) in that

— the output of our model was the summed post-synaptic potentials and not the probability of firing of neurons,

— we did not include the phenomenon of post-anodal exaltation which has been refuted on good physiological grounds (Purpura, 1970) and

— we considered the model's output under steady-state conditions with a noise input and therefore not transient responses.

The model was based on histological data from the ventro-postero-lateral nucleus of the thalamus published by Tömböl (1967). We used these histological data because these results gave the best quantitative information concerning any structure capable of generating alpha-rhythms which we had at our disposal. Two types of neurons were assumed: the thalamo-cortical relay cells or TCR neurons, and the interneurons IN. The fundamental principle of interaction between TCR and IN neurons was that a TCR would excite one or more IN neurons via a recurrent collateral of its axon. The latter, in turn, would inhibit a group of TCR neurons (negative feedback). To keep the structure as simple as possible we did not assume, at the start, the possibility of positive feedback (TCR axon collaterals exciting other TCR cells), or, of direct input to IN cells which probably exists and may play an important role as a gating mechanism for the occurrence and disappearance of alpha-rhythms.

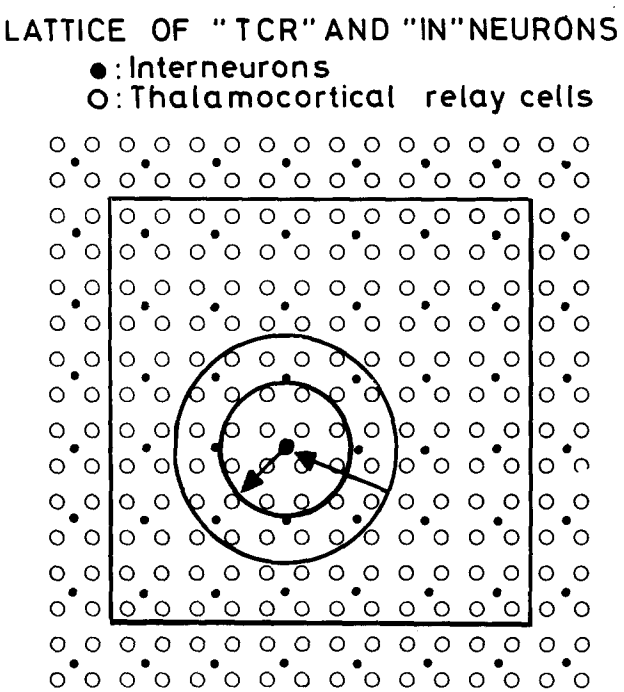

Fig. 1. The neural network simulated in the digital computer. The centripetally oriented arrow indicates the group of TCR neurons (32) which influence one IN. The centrifugally oriented arrow indicates the group of TCR neurons (12) which are under the influence of one IN

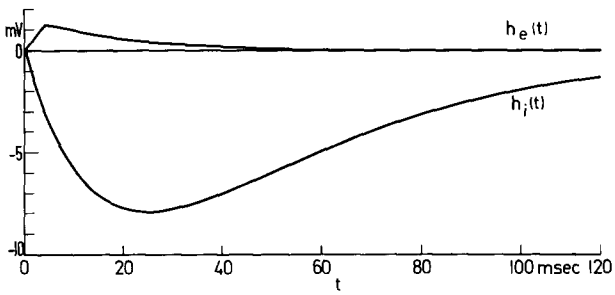

Fig. 2. Examples of schematic excitatory and inhibitory post-synaptic potentials (EPSP and IPSP). The EPSP and IPSP curves illustrated were used both in the computer simulations and in the systems analysis of the model

2.1 The Model's Structure

In the model, 144 TCR and 36 interneurons were simulated in a doublefolded matrix, i.e. in a matrix without boundaries as shown in Fig. 1. Therefore, the ratio TCR/IN neurons was 4 which agrees well with histological data (3–6 following Tömböl). The basic membrane properties of the neurons were assumed as follows:

The wave of depolarization and the wave of hyperpolarization corresponding to the excitatory and inhibitory post-synaptic potentials (EPSP and IPSP, respectively) were simulated as shown in Fig. 2.

It was assumed that the intracellular membrane potential in the resting state was -60 mV, and that this potential could not decrease in the course of hyperpolarization below -80 mV (V_{min}). A theoretical saturation level was also included so that the intracellular potential should not exceed $+30$ mV (V_{sat}).

In order to compute the membrane potential changes as a function of time, we employed simplified equations. In all computations, time was discrete in samples of 4 msec. In the model, a wave of depolarization was given by the following expression:

$$V_{i+1} = aV_i + n_i \cdot V_1 \tag{1}$$

where $n_i \cdot V_1$ is the combination of n waves of depolarization which are originated in the time unit i due to the arrival of n action potentials; a is a constant factor, $0 < a < 1$ chosen as indicated below.

The real change is, however, a function of the momentary value of the membrane potential:

$$V_{i+1} = aV_i + \frac{V_{sat} - V_i}{V_{sat}} n_i \cdot V_1 . \tag{2}$$

The constants a and V_1 are chosen so that in the case where $n_1 = 1$ and $n_j = 0 (j > 1)$, Eq. (2) gives an EPSP with the form given in Fig. 2.

If $V_1 = 1$ mV then $a = 0.7$, and one wave of depolarization (or equivalent EPSP) lasts about 30 msec. In most simulations, we took $a = 0.8$ and $V_1 = 1.2$ mV. It should be realized that a wave of depolarization represents approximately one EPSP.

For the purpose of simulating the wave of hyperpolarization, Eq. (3) was used:

$$V_{i+1} = bV_i + \frac{V_{min} - V_i}{V_{min}} \sum_{j=0}^{6} n_{i-j} \cdot V_j \tag{3}$$

where b is a constant factor, V_{min} is as defined above.

The parameters $V_j (j = 0, 1, \ldots, 6)$ are chosen so that Eq. (3) gives a good fit to the desired wave form for the hyperpolarization (equivalent IPSP). Should $b = 0.9$ and the top values of the equivalent IPSP is 8 mV, then the duration of the wave is about 100 msec.

For the general case where equivalent EPSPs and IPSPs are generated at the same time, Eqs. (2) and (3) are combined by linear summation. The remaining most important assumptions of the model are the following:

The physiological properties of TCR and IN cells were assumed to be identical due to lack of more specific knowledge. The firing threshold of both was set at 6 mV above resting membrane potential. After firing, the threshold changed up to the value of V_{sat} and decreased exponentially in order to simulate the absolute and relative refractory periods. The absolute refractory period lasted one time unit and the threshold was reset at the original value within 3 time units.

It was assumed that one IN would receive effective excitatory inputs from around a radius, r_r, of about 150 μ. Considering the known extent of the length of the dendritic arborization of these cells, which is about 250–400 μ, this appeared to give a reasonable approximation admitting a geometric scaling down factor of 2 to take into account the effective action of the input fibres. Lack of knowledge about the number and length of the TCR axon's collaterals makes it difficult to determine how many TCR cells should project upon one IN. In the model we assumed that any IN receives inputs from 32 surrounding TCR cells.

The effective radius, r_e, of one IN was assumed to be 100 μ. This implies a scaling factor of 2 since that the length of the dendrites of the TCR cells is only 200–250 μ and that the precise length of the IN axons is not known. In the model any IN projects upon 12 surrounding TCR cells. Therefore each TCR cell receives inputs from 3 IN's considering that the ratio between the number of cells TCR/IN is equal to 4.

We did not put into the model the spatial effects of the relative effectiveness of synaptic inputs as a function of their place along the somadendritic membrane.

The model had two main outputs:
the linear sum, over all cells, of the membrane potential; and the density of all action potentials leaving the network via the axons of the TCR cells.

In general, we took as the main output the sum of the membrane potential of only the TCR cells since these are the dominant components in number and size. This signal is the modelled EEG which is, therefore, assumed to be extracellular replica of the membrane potential changes as a function of time.

The input to the model was fed only to the TCR cells – at least in this phase of the research. We assumed that the input was a randomly distributed series of action potentials. The TCR cells received uncorrelated inputs. Reports of spontaneous firing in the central nervous system have shown that often these series of action potentials possess a Poisson distribution.

On the basis of the fact that one TCR cell receives about 10 extrinsic afferent fibres, we assumed that each TCR cell received 200 action potentials per second. To choose this value, we thought it useful to look for the mean rate of the spontaneous discharge occurring in optic tract fibres at rest or in darkness since eye closure provides the most conspicuous condition for the onset of alpha-rhythms.

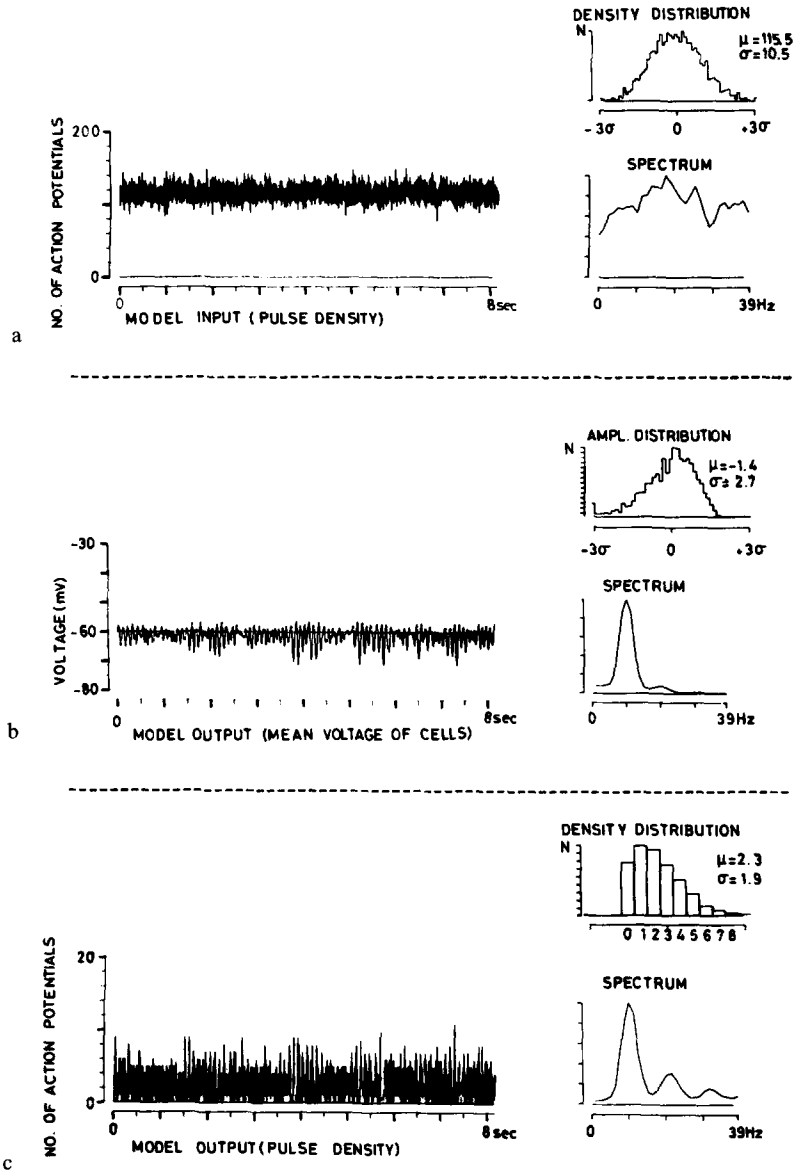

Fig. 3a–c. The input a and the two outputs of the model, namely, the summated membrane potential of the TCR neurons b and the series of action potentials fired by the TCR neurons c. At the right-hand side the amplitude distributions and the power spectrum of the three signals. The power spectrum were computed by means of the Fast Fourier Transformation, and smoothing in the frequency domain by an elliptic window. The frequency resolution is 1.2 Hz

In the literature, values around 20 action potentials per second and per fibre have been reported for the cat (Fuster *et al.*, 1965; Levick and Williams, 1964). A value of 20 action potentials per incoming fibre was, therefore, chosen for the model. Since the time unit in the model was set at 4 msec, we obtain a mean value $\mu = 0.8$ action potentials per unit time and per cell. This value was a parameter in our model, and it was only assumed that it was not likely that spontaneously active afferent fibres would have much higher rates of firing than indicated above.

Our purpose was to use the model in an attempt to answer the following question: does the simulated thalamic neural network generate a stochastic signal with characteristics analogous to alpha-rhythms when submitted to an appropriate noise input? Alpha-rhythms might then be considered as a form of filtered noise where the filter would be the thalamic network.

2.1.1. The test of the filtered noise hypothesis. When submitted to a noise with the appropriate characteristics, the model produced rhythmic oscillations of

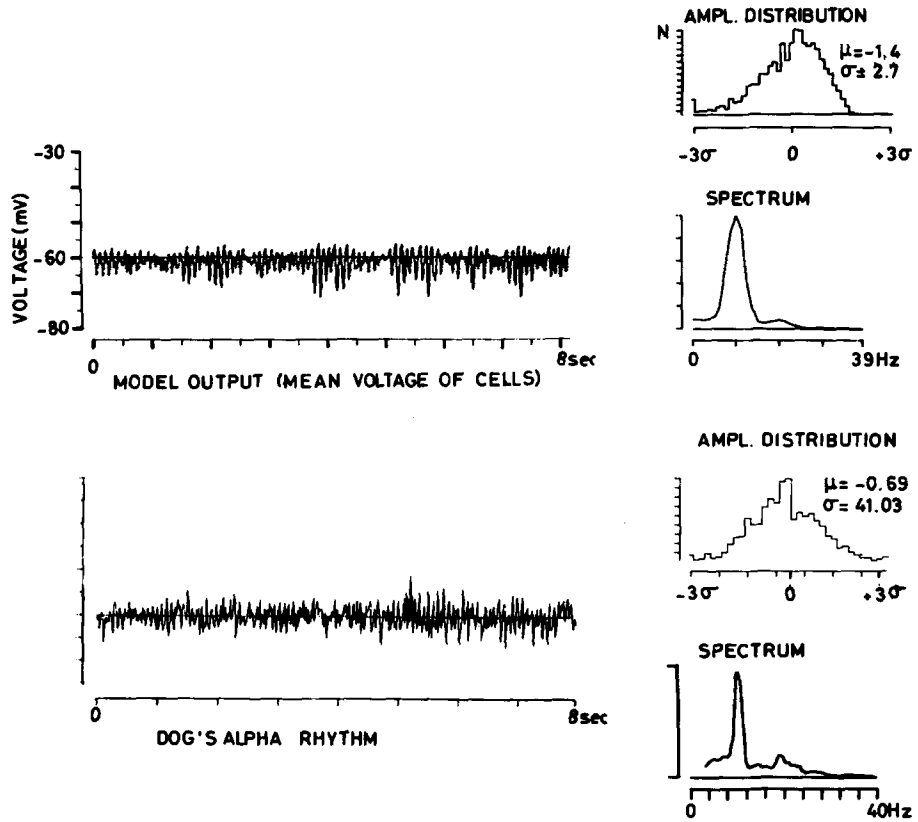

Fig. 4. Alpha-rhythm produced by the model and recorded from the occipital cortex of dog under natural conditions. At the right-hand side the corresponding amplitude distributions and power spectra (frequency resolution is 0.4 Hz for the natural alpha-rhythm and 1.2 Hz for the model's output)

potential analogous to an alpha-rhythm (see Fig. 3b). The statistical properties of these oscillatory potentials have been characterized by means of power spectra and amplitude distributions (see Figs. 3a–c). In Fig. 4 an example of dog's alpha-rhythm with corresponding amplitude distribution and power spectra is presented for comparison.

It can be seen that, in both cases, the real alpha-rhythm and the model's "alpha" present a frequency of about 9–12 Hz. The simulated alpha-rhythm waxes and wanes in amplitude, so that it may assume the form of spindles. It should be noted that the amplitude distribution is based on only a few seconds of activity due to the fact that the model output had to be kept as short as possible for technical reasons.

Without going into details of all simulations which have been done we can state that the occurrence of an alpha-rhythm, and its frequency and amplitude, were mainly dependent on the mean value of the noise input (mean rate of incoming action potentials) and on the size of the IPSP. The effect of these two parameters is shown in Figs. 5a, b. In this report we cannot deal in detail with the influence of all parameters.

In conclusion, we consider that the simulations support the hypothesis that alpha-rhythms are generated by neural networks with the characteristic of a filter and a noise input.

2.1.2. The test of the hypothesis that several noise sources contribute to thalamic and cortical alpha-rhythms and are responsible for thalamo-cortical coherences. The coherence function between two signals, $S_1(t)$ and $S_2(t)$, with estimates of power spectra $\hat{P}_1(f)$ and $\hat{P}_2(f)$ and of crosspower spectrum $\hat{G}_{1,2}(f)$ is defined as

$$\hat{\gamma}^2(f) = \frac{|\hat{G}_{1,2}(f)|^2}{\hat{P}_1(f) \cdot \hat{P}_2(f)}. \tag{4}$$

The two signals may be expressed in the following way: $S_1(t) = x_1(t) + y(t)$ and $S_2(t) = x_2(t) + y(t)$ where $x_1(t)$, $x_2(t)$ and $y(t)$ are stochastic uncorrelated signals. Accordingly the expression for the coherence between $S_1(t)$ and $S_2(t)$ can be written as follows:

$$\hat{\gamma}^2(f) = 1/[1 + (\hat{P}x_1(f)/\hat{P}y(f)) + (\hat{P}x_2(f)/\hat{P}y(f)) + \hat{P}x_1(f) \cdot \hat{P}x_2(f)/(\hat{P}y(f))^2]. \tag{5}$$

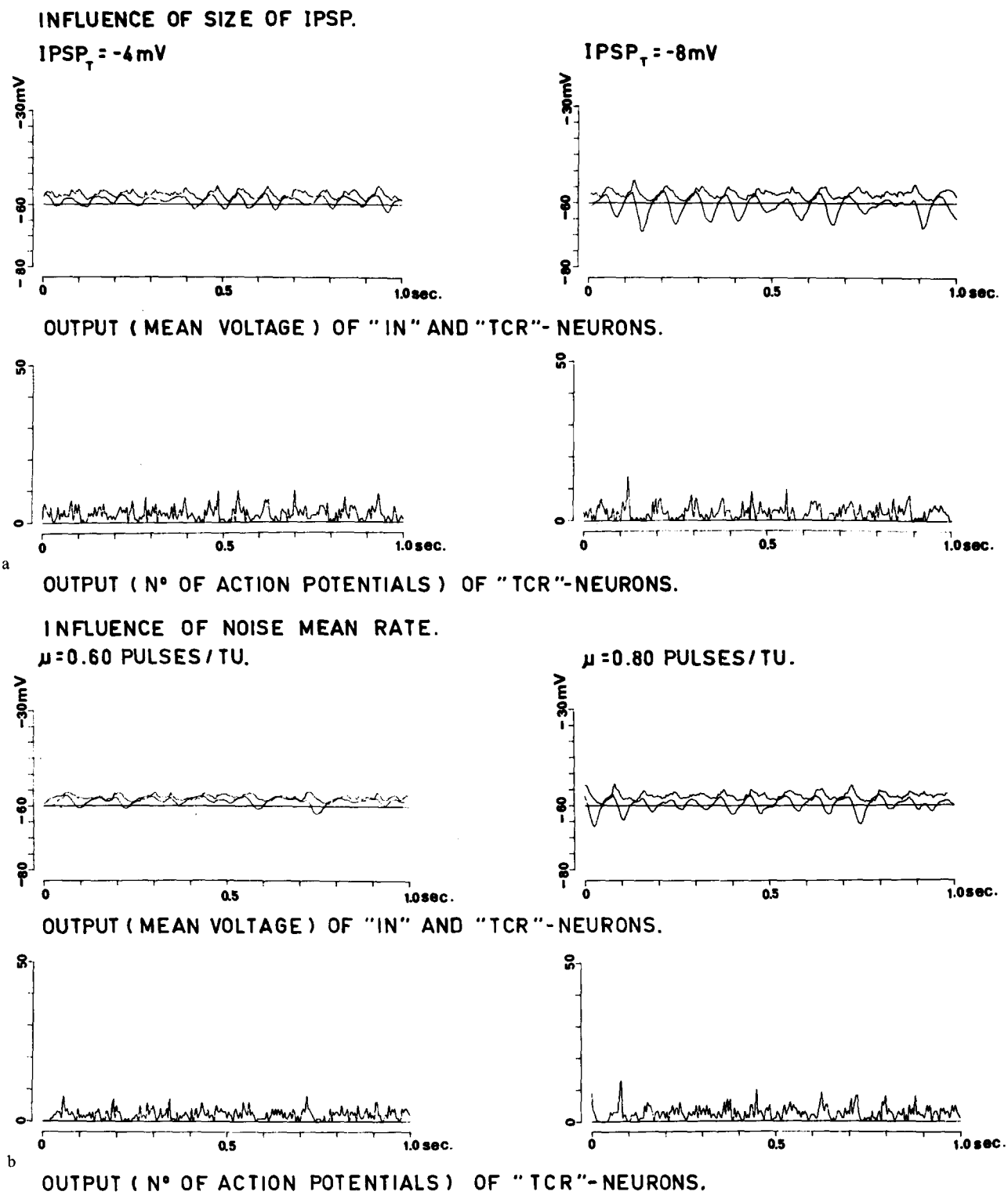

Fig. 5a, b. Influence of the size of the IPSP a and of the input noise mean rate b on the two model's outputs: The summated membrane potentials of all IN and TCR neurons and the action potentials fired by all TCR neurons. a the model outputs obtained with two different IPSP amplitudes (IPSP or top amplitude 4 mV and 8 mV) are shown: note that the rhythmicity of the membrane potentials is much stronger in the case of the larger IPSP. The two membrane potentials shown belong to the TCR and to the IN neurons; the former are the largest. b the model outputs obtained with two different levels of the mean noise input. Note that there is more rhythmicity in the case the mean pulse density is $\mu = 0.80$ pulses/time unity (4 msec) corresponding to 20 pulses/sec per input synaptic contact and to 10 input contacts per TCR neurons

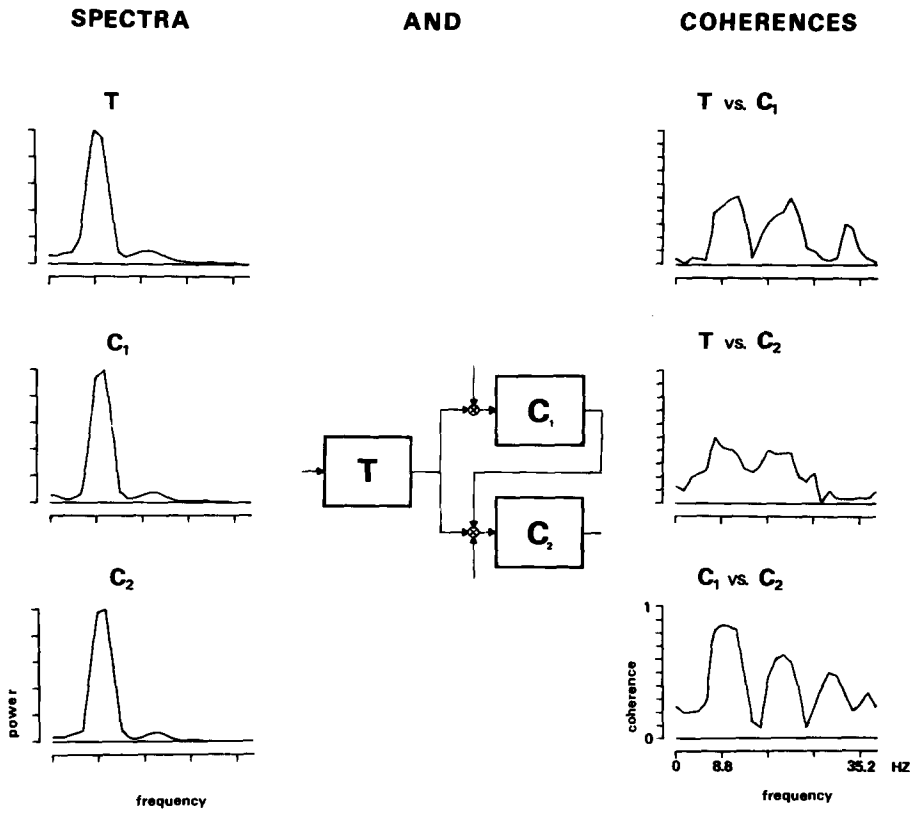

Fig. 6. Three interconnected alpha-rhythm networks. Network T simulates a central thalamic area; networks C_1 and C_2 simulate two cortical projection areas. In this simulation the output of the TCR neurons of T furnishes 8% of the action potentials forming the input of the main neurons of network C_1. These neurons receive also a superimposed but uncorrelated noise input. Network C_2 receives three inputs which are superimposed and which furnish the following contributions: 4% from T, 13% from C_1, and 83% from an uncorrelated noise source. For all the three networks the mean input is the same and equal to 200 pulses/sec per neuron. At the left-hand side the spectrograms of the alpha-rhythms generated by networks T, C_1, and C_2 are represented. The frequency scale is the same as for the coherence function on the right. The vertical scale is in arbitrary units. Note that the spectra are practically identical and that all show a peak at the alpha frequency. At the right-hand side the coherence between the three models alpha-rhythms are illustrated. Note the large coherence between C_1 and C_2 (0.85 at 10 Hz) whereas the maximal coherence between T and C_1 is only 0.5 at 12 Hz and that between T and C_2 is even only 0.49 at 8.5 Hz. The differences between the $C_1 - C_2$ coherences and the $T - C_1$ or $T - C_2$ coherences are statistically significant ($p < 0.05$)

Measurements of coherence between alpha-rhythms recorded from different areas of the brain have shown that the coherences between thalamus and cortex have a mean value of about 0.3 whereas the coherence between different areas of the cortex may reach mean values of 0.7 or 0.8 (Lopes da Silva *et al.*, 1973). In order to test whether such different values of coherence could be obtained by means of coupling different networks producing alpha-rhythms in a way analogous to the physiological case we have examined the coherence between 3 networks arranged as indicated in Fig. 6. Network 1 simulates a central thalamic area; networks 2 and 3 simulate two projection areas. In order to couple two networks it is necessary to define how the output of one is used as input of the other one. Of course the output of one network is constituted by 144 series of action potentials arising from 144 TCR cells. These series of action potentials should form the input of the 144 cells of the projection models. A basic assumption of our model is that in order to produce a good simulation of the alpha-rhythm the input of the network should have a certain mean noise level: 0.8 pulses/time unit (4 msec) per TCR neuron. The output of each TCR neuron, however, contains a much lower rate of pulses, which do not form a white noise source; on the contrary this output series has a spectrum with a peak around the alpha frequency. Since the output of TCR cells has a low density it must be complemented by adding a secondary noise source in order to form the input of the second network. The coupling between the main cells of the two networks can be thought to occur in many ways: (a) if a one-to-one correspondence between the main cells of the networks in series would be assumed, the ratio between the secondary noise source and the filtered noise coming out of the first network would become so large that no coherence would be obtained between the two networks con-

nected in series; (b) a more interesting possibility is that a group of TCR cells of the first network projects upon one cell of the second network. This gives a better ratio between the secondary noise source and the filtered noise. The main point which we wished to investigate by means of this type of simulations was whether it was possible to show that three interconnected networks may produce signals with similar spectra whereas they have significantly different degrees of coherence. In order to achieve this we set up the three-order model represented in Fig. 6. Network T, or thalamic model, was assumed as being the common input to the two networks C_1 and C_2 representing cortical projection areas. The projection of T upon C_1 was made stronger than upon C_2; four TCR neurons of T projected upon one neuron of C_1 whereas only two TCR neurons projected upon one neuron of C_2. There was, of course, overlapping between the domains of TCR neurons projecting to one neuron of C_1 or C_2 since every network was composed of the same number of neuronal elements. The secondary noise sources of the two networks (C_1 and C_2) which were necessary in order to obtain equivalent input levels, were simulated in different ways: network C_1 received only a secondary uncorrelated noise source; network C_2 received two secondary inputs, namely the output of the main neurons of network C_1 and an uncorrelated noise source.

The main results, of this simulation are illustrated in Fig. 6. They can be summarized as follows: (a) it was indeed found that the three networks produce signals with spectra which are practically identical; (b) however, the values of coherence between networks T and C_1 or C_2 were significantly lower than those found between networks C_1 and C_2. Therefore we demonstrated that such a model simulates satisfactorily the finding that the thalamo-cortical coherences are smaller than cortico-cortical coherences. The large value of the latter should be attributed to the strong interconnections between the cortical areas. It should be added that of course, we did not attempt to simulate a cortical network in its histological organization because of lack of the detailed information which is available for the thalamus. Thus the cortical model should be envisaged only as a rough approximation.

The conclusion which emerges from these simulations is that in order to obtain an alpha-rhythm in such a system of neural networks as simulated here a deterministic pacemaker is not necessary. However, the strength of coherence between different brain areas emanates from the existence of histological connections between these areas and depends (a) upon the arrangement of the neuronal projections from one area on another, and (b) on the ratio between several noise sources that they receive as inputs.

3. Systems Analysis of the Model

So far we have dealt with the alpha-rhythm model in terms of the results obtained from simulations conducted on the digital computer. It is, of course, desirable to try to generalize the model so that we may understand the influence of different parameters analytically. We have treated this problem by simplifying the model and applying a systems analysis approach. The basic treatment is inspired from the theoretical study of Wilson and Cowan (1972) and has been treated in detail elsewhere by Zetterberg (1973). The basic system to which our computer model reduces is shown in Fig. 7. The translation from the model to the scheme of Fig. 7 takes into account the following assumptions:

$E(t)$ is the proportion of excitatory cells (TCR) firing per unit of time and $I(t)$ is the proportion of inhibitory cells (IN) firing per unit of time; $P(t)$ is the pulse density fed into the excitatory subpopulation of cells; $V_e(t)$ is the average membrane potential in the excitatory population at time t and $V_i(t)$ of the inhibitory population; $f_e(x)$ and $f_i(x)$ are static functions (threshold functions) which relate the average level of the membrane potential to the pulse density of the excitatory and inhibitory cell populations, respectively; c_1 is a constant which may be inter-

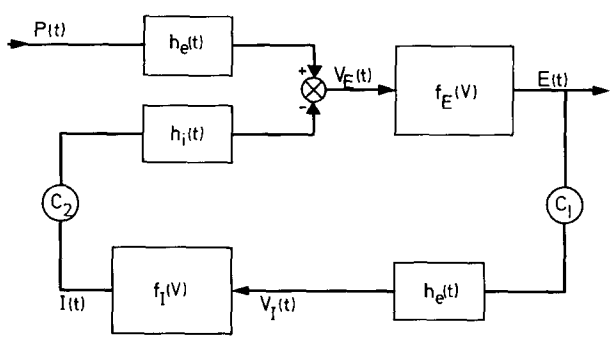

Fig. 7. Block diagram for the simplified alpha-rhythm model. The TCR neurons are represented by two input devices which have as impulse responses potentials simulating an EPSP ($h_e(t)$) and an IPSP ($h_i(t)$), respectively. Furthermore a static non-linearity $f_e(V)$ represents the spike generating process. The IN are represented only by one input element having the impulse response $h_e(t)$ and a spike generating process $f_e(V)$. The feedback from the TCR to the IN is multiplied by two factors, namely C_1 which represents the number of INs to which one TCR neuron projects and C_2 which represents the number of TCR neurons to which one IN projects

preted as the average number of synaptic contacts that the output of one excitatory cell forms and the same applies for c_2, but for one inhibitory cell; $h_e(t)$ and $h_i(t)$ are the impulse responses for the excitatory and inhibitory synapses. They may be viewed as the equivalent to an excitatory postsynaptic potential (EPSP) or an inhibitory postsynaptic potential (IPSP). The non-linearity introduced by $f_e(x)$ and $f_i(x)$ is given in the following expressions:

$$E(t) = f_e[V_e(t)] \tag{6}$$

$$I(t) = f_i[V_i(t)] \tag{7}$$

$f_e(x)$ and $f_i(x)$ are monotonously increasing and hence they have unique inverses. Thus we may write

$$V_e(t) = f_e^{-1}[E(t)] \tag{8}$$

$$V_i(t) = f_i^{-1}[I(t)]\,. \tag{9}$$

The four stochastic processess $E(t)$, $I(t)$, $V_e(t)$, and $V_i(t)$ are defined as spatial averages over a fairly large population of cells. Hence it may be expected that at a fixed time the standard deviations of these quantities are small compared to the mean values. For intermediate level of excitation it is reasonable to assume that the two functions $f_e^{-1}(y)$ and $f_i^{-1}(y)$ may be expanded in a Taylor series around the mean value $\bar{E}$

$$f_e^{-1}[E(t)] = a_{e0}(\bar{E}) + a_{e1}(E(t)-\bar{E}) + a_{e2}(E(t)-\bar{E})^2 + a_{e3}(E(t)-\bar{E})^3 \tag{10}$$

and similarly for $f_i^{-1}[I(t)]$. Here only the two first terms will be taken into account. But basically we are not interested in mean values but rather on variations around the means of the stochastic processes $E(t)$, $I(t)$, $P_i(t)$ and $V_e(t)$.

Therefore it is convenient to introduce the processes:

$$\begin{aligned} e(t) &= E(t) - \bar{E} \\ i(t) &= I(t) - \bar{I} \\ p(t) &= P(t) - \bar{P} \\ v_e(t) &= V_e(t) - \bar{V}_e \\ v_i(t) &= V_i(t) - \bar{V}_i\,. \end{aligned} \tag{11}$$

We can now write the equations governing the operations indicated in the scheme of Fig. 7 applying Laplace transforms:

$$P(s)\,H_e(s) - C_2 I(s)\,H_i(s) = a_{e1} E(s) = V_e(s) \tag{12}$$

and

$$C_i H_e(s)\,E(s) = a_{i1} I(s) = V_i(s) \tag{13}$$

where $P(s)$, $E(s)$, $I(s)$, $H_e(s)$, $H_i(s)$, $V_e(s)$ and $V_i(s)$ are the Laplace transform of $p(t)$, $e(t)$, $i(t)$, $h_e(t)$, $h_i(t)$, $v_e(t)$, and $v_i(t)$ respectively.

Combining expressions (12) and (13) we obtain the expression for $V_e(s)$:

$$V_e(s) = \frac{P(s)\,H_e(s)}{1 + \dfrac{C_1 C_2 H_i(s)\,H_e(s)}{a_{i1} a_{e1}}} \tag{14}$$

setting

$$\frac{1}{a_{i1}} = q_{i1} \quad \text{and} \quad \frac{1}{a_{e1}} = q_{e1}$$

where q_{e1} represents the slope of the function f_e at $\bar{E}$ which gives the relationship between the number of excitatory cells firing per unit of time $[E(t)]$ and the membrane potential $V_e(t)$; for q_{i1} the same holds for the inhibitory cells.

We get

$$V_e(s) = \frac{P(s)\,H_e(s)}{1 + C_1 C_2 q_{e1} q_{i1} H_i(s)\,H_e(s)}\,. \tag{15}$$

At this stage we must make some assumptions about the transfer functions $H_i(s)$ and $H_e(s)$ which have impulse responses equivalent to the inhibitory (IPSP) and excitatory (EPSP) post-synaptic potentials, respectively. These transfer functions may be approximated by second order systems. The corresponding impulse responses constitute an approximation of the real post-synaptic potentials which are shown in Fig. 2. In this case the impulse responses are given by the expressions,

$$h_i(t) = B[\exp(-b_1 t) - \exp(-b_2 t)] \tag{16}$$

$$h_e(t) = A[\exp(-a_1 t) - \exp(-a_2 t)] \tag{17}$$

with $a_2 > a_1$ and $b_2 > b_1$.

The corresponding transfer functions are then

$$H_i(s) = \frac{(b_2 - b_1)\,B}{(s+b_1)(s+b_2)} \tag{18}$$

and

$$H_e(s) = \frac{(a_2 - a_1)\,A}{(s+a_1)(s+a_2)}\,. \tag{19}$$

The values of a_1, a_2, b_1, b_2, A and B which were used in the present simulations are given below.

Including these expressions in (15) and setting

$$C_1 C_2 q_{e1} q_{i1} (a_2 - a_1)(b_2 - b_1)\,AB = K \tag{20}$$

we get

$$V_e(s) = \frac{(a_2 - a_1)\,AP(s)(s+b_1)(s+b_2)}{(s+a_1)(s+a_2)(s+b_1)(s+b_2) + K}\,. \tag{21}$$

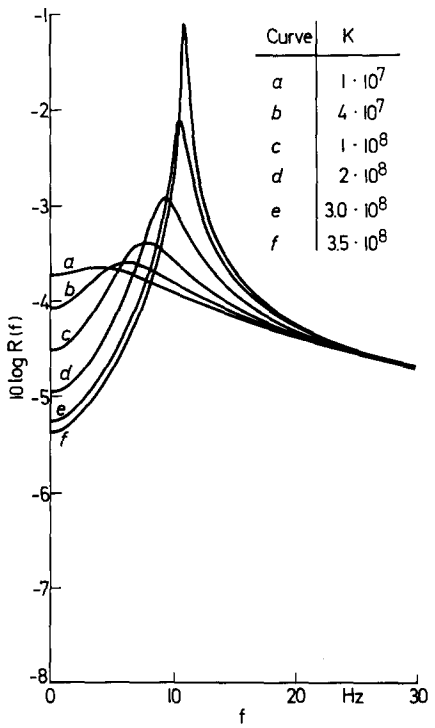

Fig. 8. The influence of the feedback factor K (for explanation see text) on the spectrum of the model's output. Note that if K is small the spectrum is predominantly that of a low pass filter; as K increases the spectrum acquires a clear selectivity at the alpha-frequency

In the constant K there are several factors; the coupling constants C_1 and C_2; the threshold functions q_{e1} and q_{i1} and the parameters of the synaptic responses.

If the coupling within the network is very small than K is negligible and the transfer function of the network expressed as

$$g_p(s) = V_e(s)/P(s)$$

approaches the transfer function for the EPSP.

As the coupling constant K increases complex poles will originate. This is the most interesting case for understanding the generation of rhythmic activity. As K increases still more some poles will move into the right half plane ($\sigma > 0$) and the network will become unstable.

The power spectrum of $V_e(t)$ may be obtained from expression (21) substituting s by $j\omega$ and assuming that $P(s)$ is a constant since the spectrum of the input noise is flat.

The influence of K on the power spectrum of $V_e(t)$ is shown in Fig. 8 for values of K corresponding to stable solutions.

We shall consider how these values were numerically accounted for. The numerical values of the constants representing the synaptic potentials (see Fig. 2) were such that

$$(a_2 - a_1)(b_2 - b_1)\, AB = 0.801 \quad \text{in} \quad V^2/\text{sec}^2$$

with $a_1 = 55$, $a_2 = 605$, $b_1 = 27.5$, and $b_2 = 55$ in sec^{-1}. The constants A and B were calculated as indicated below; the EPSP has a top value of 1.2 mV so that $A = 1.65$ mV and the IPSP has a top value of 8 mV so that $B = 32$ mV.

For C_1 and C_2 we used the values obtained from the simulations described in the preceding section; C_1 is the number of TCR cells which project upon one IN and was set equal to 32; C_2 was the number of IN which project upon one TCR and was equal to 3. Thus in order to get a value of $K = 3.5 \times 10^8$ which corresponds to the maximum in the spectrum we have that $q_{e1} q_{i1} = 4.55 \times 10^6$. That value of K is close to the stability limit of the network.

Considering for simplicity that $q_{e1} \approx q_{i1}$ which is the case in our computer simulations we have that $q_{e1} \approx 2130$ which represents that, theoretically, 2.1 cells would fire, per sec., as the average membrane potential of the cell population increases by 1 mV. This has been confirmed in the computer network simulations; it should now be confirmed experimentally.

One of the very interesting aspects which emerged from the model's system analysis is the study of the influence of K. Indeed it is curious to note that the family of spectra of Fig. 8 approximates the development of the EEG as function of age; in this way we have obtained a useful model of the *development of the* EEG. Considering that it is likely that the threshold parameters, q_{e1} and q_{i1} should not change much and the synaptic time constants only slightly, it follows that the main parameter which should change during development would be C_1 and C_2 i.e. the coupling constants. Therefore it may be seen that the development of the EEG from a predominantly low frequency spectrum signal to a signal with a clear rhythmic component would depend upon an increase in interconnections and synaptic contacts.

In conclusion the systems analysis of the model enables us to evaluate the influence of different parameters upon the statistical properties of the resulting rhythmic activity in an analytical form, which is simpler than the computer simulations. Furthermore it enables us to generalize the model to other forms of cooperative processes in neural systems.

Acknowledgements. We wish to thank Ir. M. ten Hoopen and Drs. A. van Rotterdam for reading the manuscript and discussing it.

References

Andersen, P., Gillow, M., Rudjord, T.: Rhythmic activity in a simulated neuronal network. J. Physiol. (Lond.) 418—428 (1966)

Fuster, J. M., Herz, A., Creutzfeldt, O. D.: Interval analysis of cell discharges in spontaneous and optically modulated activity in the visual system. Arch. ital. Biol. **103**, 159—177 (1965)

Lopes da Silva, F. H., Van Lierop, T. H. M. T., Schrijer, C. F., Storm van Leeuwen, W.: Organization of thalamic and cortical alpha rhythms: spectra and coherences. Electroenceph. clin. Neurophysiol. **35**, 627—639 (1973)

Levick, W. R., Williams, W. O.: Maintained activity of lateral geniculate neurons in darkness. J. Physiol. (Lond.) **170**, 582—597 (1964)

Purpura, D.: Operations and processes in thalamic and synaptically related neural subsystems. In: Schmitt, F. O. (Ed.): The Neurosciences. Vol. 2, pp. 458—470. New York: Rockefeller Univ. Press 1970

Rashevsky, N.: A note on nonperiodic undamped oscillations with special reference to brain waves. Bull. Math. Biophys. **33**, 281—293 (1971)

Saunders, M. G.: Amplitude probability density studies on alpha and alpha-like patterns. Electroenceph. clin. Neurophysiol. **15**, 761—767 (1960)

Tömböl, T.: Short neurons and their synaptic relations in the specific thalamic nuclei. Brain Res. **3**, 307—326 (1967)

Wilson, H. R., Cowan, J. D.: Excitatory and inhibitory interaction in localized populations of model neurons. Biophys. J. **12**, 1—23 (1972)

Zetterberg, L. H.: Stochastic activity in a population of neurons – a system analysis approach. Report Inst. Med. Physics TNO, Utrecht, **1**, 153 (1973)

Dr. F. H. Lopes da Silva
Institute of Medical Physics TNO
Da Costakade 45
Utrecht, The Netherlands